Semiconductor Physics, Quantum Electronics & Optoelectronics, 2021. V. 24, No 3. P. 304-311.

Optics

The approaches for localized surface plasmon resonance wavelength position tuning. Short review

P.V. Demydov[1], A.M. Lopatynskyi[1,2], I.I. Hudzenko[1] and V.I. Chegel[1,2]

[1]*V. Lashkaryov Institute of Semiconductor Physics, 03028 Kyiv, Ukraine*
[2]*Institute of High Technologies, Taras Shevchenko National University of Kyiv,*
64/13, Volodymyrska str., 01601 Kyiv, Ukraine
Corresponding author e-mail: *vche111@yahoo.com*

Abstract. A unique feature of nanoparticles made from highly conductive materials (plasmonic nanoparticles) is that their localized surface plasmon resonance (LSPR) wavelength position can be tuned by changing the shape, size, composition and environment in accordance with the purpose of the application. In this paper, the main mechanisms of LSPR tuning that are available at the present time are reviewed. In particular, a widely used method for tuning the LSPR wavelength position is based on selecting the type of a plasmonic nanoparticle material such as gold, silver, copper, aluminum and gold-silver alloy. The examples of changing the resonance absorption position by using nanoparticles with different shapes and dimensions have been also demonstrated. Furthermore, works with less used LSPR tuning methods, such as controlled regulation of the distance between nanoparticles in one and two dimensions have been considered. The number of works is given, where the LSPR wavelength position can be also controlled by changing the environment in the vicinity of plasmonic nanoparticle: the substrate thickness, the thickness and dielectric parameters of the layer on the surface of the nanoparticle. Examples of active influence on the change in the wave position of LSPR by applying an electric potential and regulating plasma modes have been also discussed.

Keywords: localized surface plasmon resonance, gold nanostructures, nanochip, LSPR tuning.

https://doi.org/10.15407/spqeo24.03.304
PACS 73.20.Mf, 78.67.Bf, 78.67.-n, 81.07.-b

Manuscript received 20.05.21; revised version received 12.07.21; accepted for publication 18.08.21;

1. Introduction

Surface plasmon resonance (SPR) has a special place among modern scientific techniques that combine the possibilities for research in materials science, bio- and chemosensorics [1, 2]. Surface oscillations of free electrons in highly conductive materials (surface plasmons) during their resonant excitation by light create a sensitive electromagnetic field that penetrates the nearby environment and can be used as an active supersensitive probe to the changes in its refractive index. The non-destructive nature of the surface plasmon field makes it possible to study biomolecules in their natural state without the use of various kinds of labels in real time [3].

Due to the significantly high sensitivity of LSPR to the changes in the refractive index of the environment near the surface of plasmonic nanoparticles, the most common application of this phenomenon is creation of sensitive elements for sensors [4, 5]. When studying the molecules that have their own light absorption peak with a LSPR sensor, the spectral position of the LSPR peak relative to the absorption peak of an optically active molecule affects the sensor signal, which can be either weakened or enlarged as a result [6].

Depending on the purpose of experiments, a sensitive element ought to exhibit the absorption of light in a certain spectral range. Thus, plasmonic nanoparticles in combination with infrared radiation are used to study and treat cancer cells [7–9]. Accordingly, it becomes

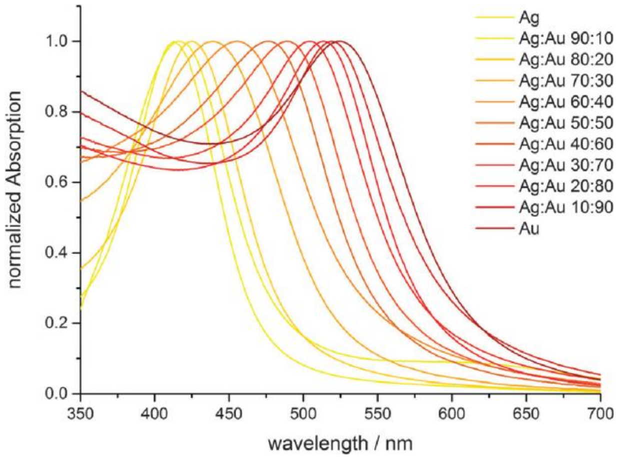

Fig. 1. LSPR absorption spectra for nanoparticles of gold, silver and gold-silver alloy [16].

necessary to modify nanoparticles to shift their absorption spectrum to the near infrared range. In addition, fluorescence microscopy can be used to study organs and tissues [10], which also requires operating with certain wavelengths from fluorophore labels. This can be achieved by creating a complex of fluorophores and nanoparticles. In addition to biomedical applications, plasmonic nanoparticles are also used in photovoltaics to enhance light absorption [11]. In this case, the LSPR wavelength position of the nanoparticles should correspond to a certain absorption wavelength of the photovoltaic element. Another use of nanoparticles is to enhance the fluorescence of various fluorophores, including quantum dots [12]. However, for achieving amplification it is necessary that the luminescence spectrum of the fluorophore overlaps with the absorption spectrum of the nanoparticle, which also requires regulation (tuning) of the LSPR wavelength position of the nanoparticle. Based on the said above, it is obvious that nanoplasmonic chips and colloidal solutions of nanoparticles with a fixed LSPR wavelength position can be used only for certain applications, and LSPR tuning is an actual task.

However, at present there is no single universal way to tune the LSPR wavelength position of plasmonic nanoparticles. This work describes the currently available approaches for tuning the LSPR wavelength in order to understand and generalize the modern capabilities of sensitive elements based on the phenomenon of localized surface plasmon resonance.

2. Different materials

Despite the fact that silver and gold are the most common materials for plasmonic nanoparticles, LSPR excitation is theoretically possible in any metal, alloy, or semiconductor with a negative real part and a small value of the imaginary part of the material dielectric constant [13, 14]. Gold nanoparticles with a size of about 10 nm exhibit resonant absorption at the wavelength close to 520 nm [15]. The study of the gold-silver alloy shows an absorption peak with a variable wavelength depending on the gold-silver ratio [16]. The absorption spectra for gold, silver and gold-silver alloy are shown in Fig. 1 [16].

Other materials, such as aluminum, potentially offer advantages in sensor sensitivity, the use of various surface coatings, and LSPR in the ultraviolet range, where many organic molecules absorb light [17].

Studies show that nanoparticles with the same shape (nanopyramids) and dimensions (width 390 nm, height 50 nm) and under the same conditions (glass substrate, nanoparticles surrounded by nitrogen) exhibit the wavelength position and width of the LSPR peaks which are different for various materials. For nanoparticles made of aluminum, silver, copper and gold, the wavelengths of resonance absorption peaks are 508, 639, 698 and 787 nm, accordingly. The peak halfwidths are ~ 0.65, ~ 0.29, ~ 0.36, and ~ 0.40 eV, respectively [18] (Fig. 2).

3. Shape and size

LSPR wavelength can be modified during fabrication of plasmonic nanostructures by controlling the shape and size parameters of various chemical processes during synthesis and lithographic techniques. For example, an array of triangular nanoprisms can be fabricated by nanosphere lithography [19]. During preparation of nanoparticles with a triangular pyramid shape, it is possible to further change their size and shape by electrochemical etching. To do this, studies were performed with silver nanopyramids deposited on an electroconductive substrate made of indium-tin oxide (ITO) [20]. Gradually, the electrochemical potential was changed resulting in electric charge transfer ranging from 10 to 1000 μC, etching the nanopyramids during the process and changing their shape from triangular (with LSPR wavelength position of 782 nm) to cylindrical (with LSPR wavelength position of 426 nm) (Fig. 3).

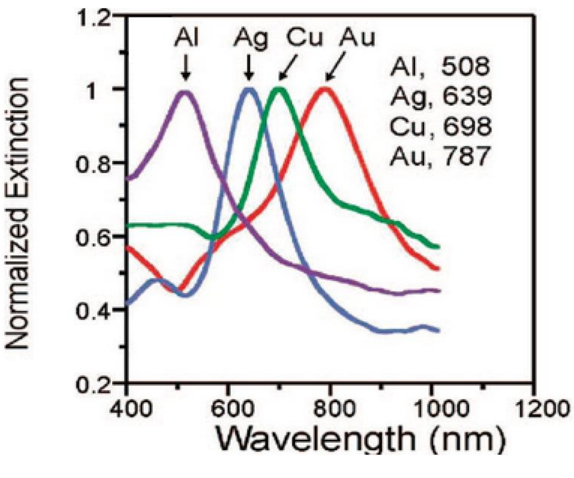

Fig. 2. Normalized extinction spectra for pyramidal nanoparticles of aluminum, silver, copper and gold of the same shape, size and under the same conditions (width 390 nm; height 50 nm; glass substrate; N_2 environment) [18].

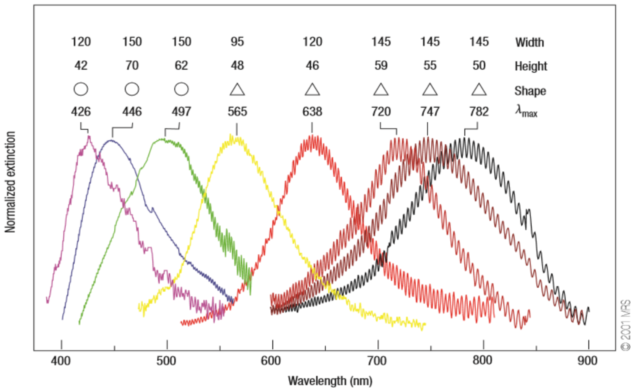

Fig. 3. Dependence of LSPR wavelength position on the shape and size of nanoparticles [20].

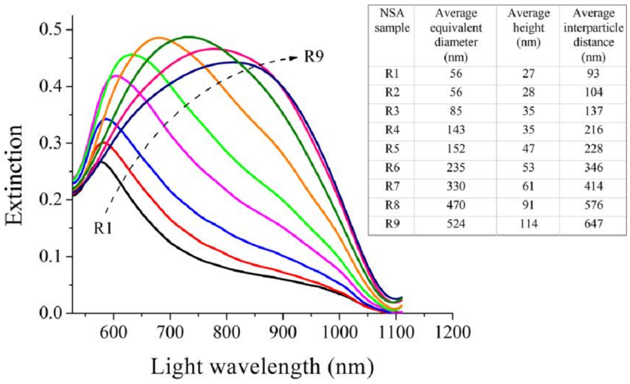

NSA sample	Average equivalent diameter (nm)	Average height (nm)	Average interparticle distance (nm)
R1	56	27	93
R2	56	28	104
R3	85	35	137
R4	143	35	216
R5	152	47	228
R6	235	53	346
R7	330	61	414
R8	470	91	576
R9	524	114	647

Fig. 4. Measured extinction spectra of gold nanostructure array (NSA produced via thermal annealing of gold island films. Normal incidence unpolarized light extinction spectra for samples R1 to R9 with different initial gold island film thickness exhibit peaks located in the wavelength range from 576 to 809 nm. Inset: the table with respective geometrical parameters of nanostuctures arrays [21].

The authors [21] show thermal annealing (450 °C) of gold island film with different thickness as possible approach for LSPR tuning. It was found that the peak position in the unpolarized light extinction spectrum, which corresponds to the occurrence of LSPR, shifts towards longer wavelengths with an increase in the initial gold island film thickness. The direct relation between lateral dimensions and height of nanostructures produced after annealing, and the initial gold island film thickness was revealed. Thus, it is possible to tune the LSPR spectral position in the wavelength range from 576 to 809 nm (Fig. 4) by changing the initial gold island film thickness.

As the size of plasmonic nanospheres increases, a redshift is observed due to the electromagnetic delay in larger particles. Thus, for a silver nanoparticle with a size of 30 nm, resonance is observed at the wavelength close to 390 nm, while nanoparticles with the size of 60 nm have the peak at 480 nm [22]. However, size tuning techniques are very limited. In many biological applications (especially *in vivo*), it is desirable to work with the near infrared range 650…900 nm. One of the ways to tune the LSPR position to the longer wavelengths is to change the nanoparticle shape from spherical to the elongated, ellipsoidal shape. These nanoparticles, in contrast to the spherical ones, have two resonances due to the plasmonic oscillations along the short and long axes [23]. The total resonance depends on the ratio of the length of the long axis to the short one (Fig. 5). Obtaining elongated nanostructures in colloidal solutions is not difficult, whereas fabrication of nanochips with nanostructures of such geometry requires lithographic methods.

4. Distance between nanoparticles

For the complex nanoplasmonic structures consisting of several closely located nanoparticles, collective surface plasmon resonance is a typical phenomenon. In such a system, the surface plasmon resonances of all elements are interrelated, forming collective modes that can be localized throughout the structure.

The unique feature of the collective plasmon mode resonance is the fact that as the distance between the particles increases, it gradually transforms from a quadrupole component into separate nanoparticles that do not interact with each other (Fig. 6). As the distance between the nanoparticles decreases, the intensity of the interaction of quadrupole modes increases significantly, while the dipole interaction almost disappears [24].

Collective plasmon modes open up new possibilities for the use of interactions between nanostructures, for example, such a system is an excellent candidate for mechanical tuning of the resonant peak wavelength position. The authors [24] created a structure in the form of an array of silver nanoparticles in the elastic layer of PDMS and investigated the possibility of tuning the nanoplasmonic resonance wavelength position due to mechanical tension. As a result of this experiment, the light extinction spectra for different degrees of stretching of the elastic substrate were demonstrated to be highly sensitive to the interparticle distance (Fig. 6).

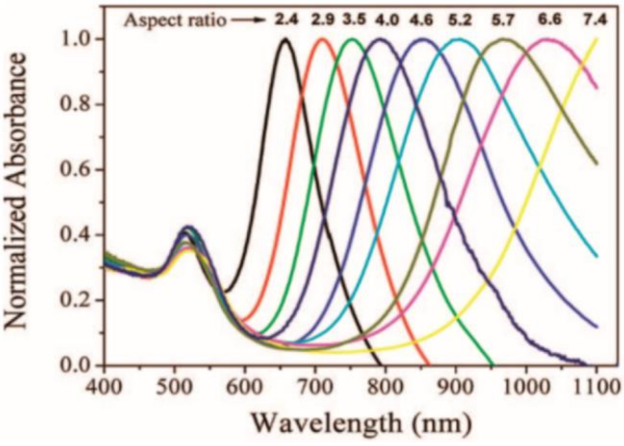

Fig. 5. UV-vis absorption spectra of nanoparticles with an aspect ratio of 2.4 to 7.4 [23].

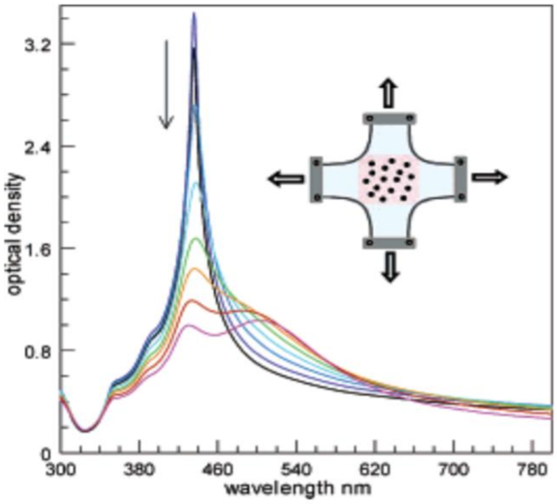

Fig. 6. Extinction spectra of a 2D array of silver nanoparticles in the PDMS layer. The red curve corresponds to a film stretch of 50% relative to the original size (black curve). The insert shows a schematic representation of the tension along these two axes [24].

5. Change of the thickness of surrounding layer

One of the most common methods of regulating the LSPR wavelength position is to influence the environment of the nanoparticle in order to change its properties. Thus, it was shown that the change in the thickness of the layer on the surface of the nanoparticle shifts its absorption spectrum [25]. TiO_2 or SiO_2 coated gold nanorods were used in the experiment. LSPR spectra of pure and coated gold nanorods with different coating thickness are shown in Fig. 7. The left and right parts of Fig. 7 correspond to the transverse and longitudinal modes, respectively. For the longitudinal mode, there is a shift of the LSPR peak towards larger wavelengths with increasing coating thickness. For the transverse mode, there is also a shift of the LSPR extinction peak towards greater wavelengths with increasing thickness, but the shift rate is much lower as compared to the longitudinal mode.

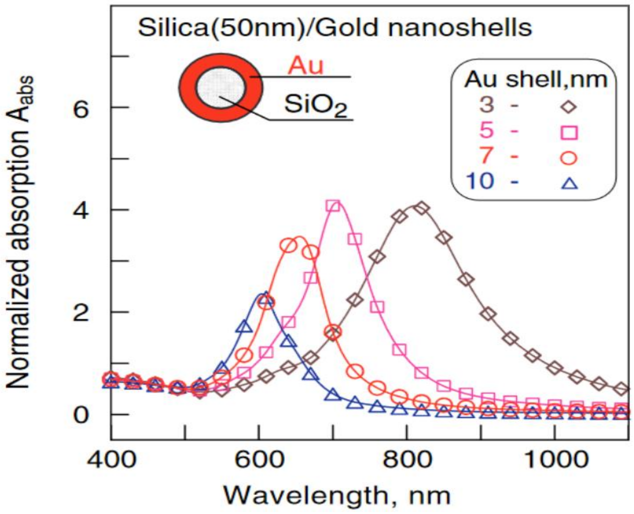

Fig. 8. UV-vis extinction spectra for nanostructures of the core SiO_2 – gold shell type. The diameter of the silica core for all curves is 50 nm, the thickness of the gold layer varies from 3 nm (black curve ◊) to 10 nm (blue curve Δ) [26].

In the next research, the effect of the thickness of the gold layer on the surface of a spherical SiO_2 nanoparticle with a diameter of 50 nm was investigated [26]. The thickness of the gold layer varied from 3 nm to 10 nm. According to the spectra in Fig. 8, as the thickness of the gold layer increases, the peak of the extinction spectrum blueshifts from 820 nm for a 3-nm-thick gold shell to 600 nm for a 10-nm-thick gold shell.

6. Change of the composite matrix structure

The authors of [27] demonstrated a plasmonic nanocomposite matrix film with LSPR spectrum that can be adjusted by UV radiation. Silver ions are added to polyacrylic acid (PAA), and in a resulting nanocomposite matrix PAA acts as a reinforcing material and silver as a functional element. Under the action of UV radiation, silver ions were reduced to silver nanoparticles.

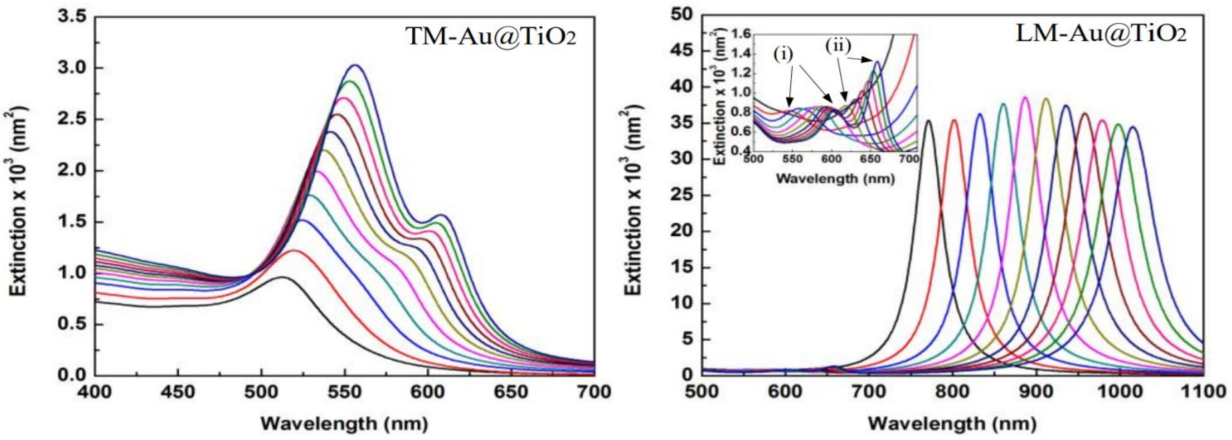

Fig. 7. Extinction spectra of gold nanorods coated with TiO_2 layer depending on the thickness of the TiO_2 layer in the longitudinal (LM) and transverse (TM) modes. In the insert, figures (i) and (ii) reflect interband transitions such as quadrupole and hexapol modes, respectively [25].

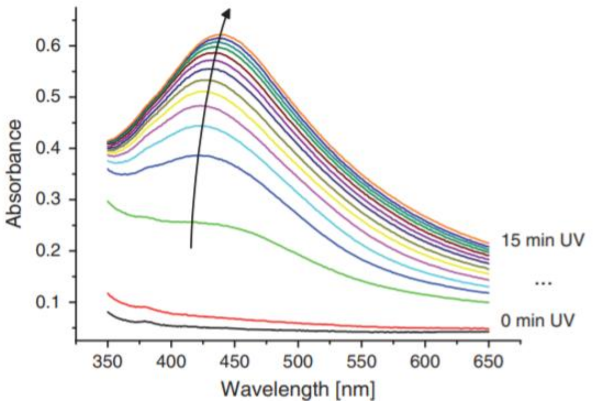

Fig. 9. The absorption spectrum of the PAA film during 15 min of irradiation with UV light, which leads to the appearance of silver nanoparticles embedded into the composite matrix accompanied by the absorption peak shift from 420 to 440 nm with a significant increase in peak intensity [27].

The irradiation time allowed controlling the concentration and, accordingly, the distance between the silver nanoparticles. Fig. 9 shows the change in the LSPR peak wavelength position of the nanocomposite matrix film for 15 min. The peak shifted from the initial wavelength of 420 nm to the final one of 440 nm.

7. Interference of plasmon modes

LSPR position tuning experiments were also performed with gold nanoparticles in the shape of a star that consist of a sphere and tips emanating from the sphere [28]. These Au nanoparticles have two LSPR modes that correspond to the field localization on the central nucleus and on the tips. The low-energy mode is strongly localized on the tips, which has been demonstrated by electron energy loss spectroscopy (EELS) and theoretical modeling. Initially, the prepared colloidal solution of nanoparticles exhibited a well-defined LSPR band with maximum absorption at 781 nm (tip mode) together with a weaker shoulder at about 545 nm, which corresponds to the mode of the central nucleus of nanoparticle. Aqueous dispersions of PVP-coated Au nanoparticles were prepared and mixed with cetyltrimethylammonium bromide (CTAB). Fig. 10 shows the evolution of UV-Vis-NIR spectra during the CTAB-induced reshaping process, revealing a continuous blue shift of the LSPR for the tip mode over time during which it almost completely (530 min) merges with the high-energy mode resembling the spectrum of Au spheroids. TEM characterization at intermediate stages (0, 60, 120, 180 and 240 min) reveals the process of shape change (Figs 10b and 10c), when spherical nanoparticles with sharp tips are almost completely transformed into smooth spherical nanoparticles [28].

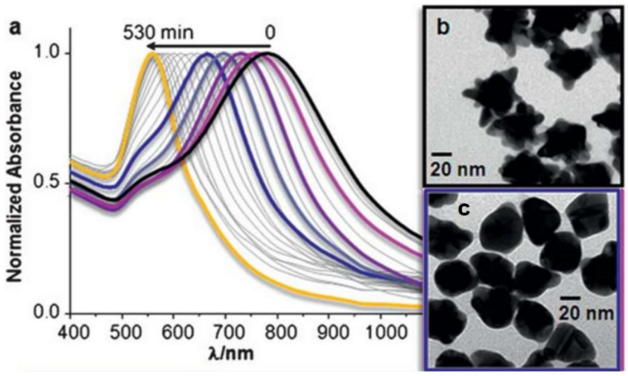

Fig. 10. (a) Spectral evolution over time of the colloidal solution of star-shaped Au nanoparticles in the presence of 0.1 mM CTAB. (b, c) TEM images of star-shaped Au nanoparticles before mixing with CTAB (b) and after 240 min (c) [28].

8. Active plasmonic devices

In the paper [29], it was shown that LSPR phenomenon in the array of gold nanoparticles can be controlled, switched and modulated by electrochemical transformation of the conductive polymer between the reduced and oxidized states. This active plasmonic device consists of an ITO substrate, polyaniline (PANI) as a conductive polymer and an array of gold nanoparticles. Gold nanoparticles were chosen because of their ability to rapidly transit from the reduced nonconductive state to the oxidative conductive state, which allows them to be used as quick switches. In addition, the PANI layer can withstand more than 10^5 switches without signs of degradation of the electrochemical signal. Fig. 11 shows the absorbance spectra of an array of gold nanoparticles in water, air, and with the PANI layer in the reduced and oxidized states.

Several groups of authors show that wide range of LSPR tuning is possible when optically active molecules are adsorbed on the surface of plasmonic nanoparticles [30–32]. The tuning of LSPR position in this case

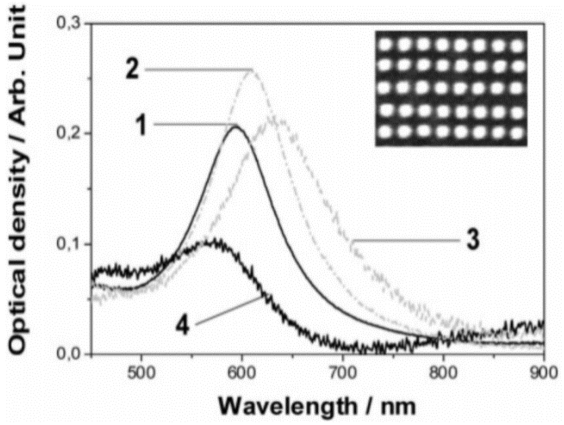

Fig. 11. Absorbance spectra of an array of gold nanoparticles (diameter = 150 nm, height = 40 nm). The distance between the nanoparticles along the *x* and *y* axes is 220 nm: (1) in air, (2) in water, (3) with a 100-nm-thick PANI layer in the reduced state, and (4) with a 100-nm-thick PANI layer in the oxidized state. Insert: SEM image of an array of nanoparticles [29].

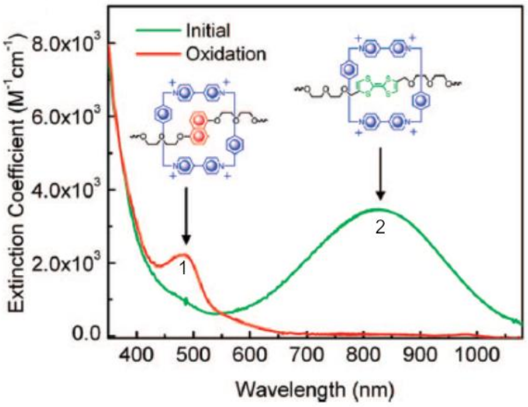

Fig. 12. The extinction spectra of rotaxane before (green line) and after (red line) oxidation of $Fe(ClO4)_3$ in DMF (0.05 mM) [30].

depends on the spectral overlap between the resonant positions of nanoparticle and adsorbed redox molecule. Authors [30] demonstrate a molecular-level plasmonic switch of bistable rotaxanes immobilized on the surface of Au nanodisks that can be chemically reversibly controlled. When stimulated by chemical reagent ($Fe(ClO4)_3$), such approach allows significant LSPR wavelength shift (480 up to 830 nm) between oxidized and reduced states of the molecule (Fig. 12).

It is also worth noting that a highly ordered array of Au/Ag nanodomes can be used for LSPR tuning in the wavelength range from 430 up to 650 nm [33]. The structure consists of a gold nanoparticle as a core and a layer of silver, which is formed due to the deposition of silver ions under the influence of an electric field. LSPR regulation is achieved due to electrochemical deposition or removal of nanoparticles, depending on the sign of the applied field and the time of action of the field. Accordingly, the size and shape of the nanoparticles changes, which affects their optical properties. Fig. 13 shows the reflectance spectrum of an array of ordered nanodomes depending on the electrochemical deposition time.

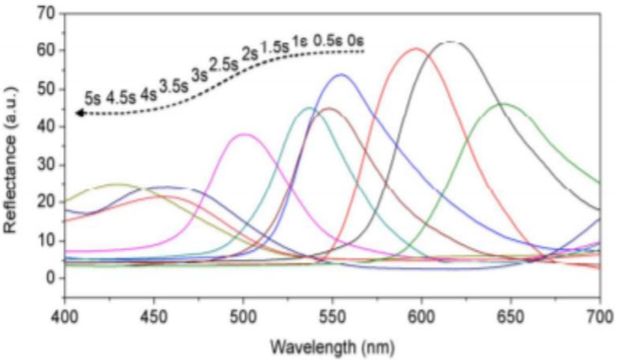

Fig. 13. The reflectance spectra of an array of nanoparticles with a gold core and a silver layer on the surface of the core, depending on the time of electrochemical deposition [33].

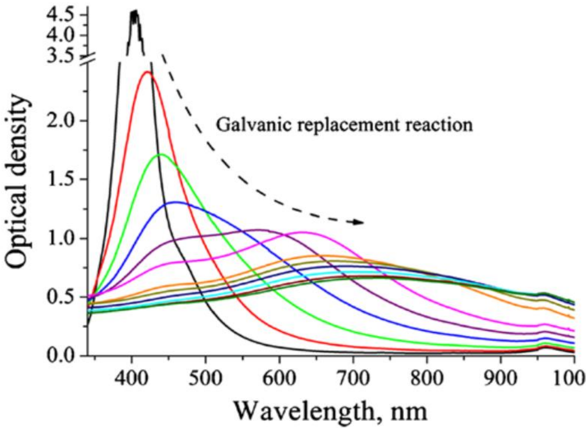

Fig. 14. Evolution of spectral properties of nanostructure colloidal solution during the galvanic replacement reaction [34].

The authors [34] demonstrated the LSPR wavelength tuning by the growth of gold layer on the surface of silver nanoparticles during galvanic replacement reaction between silver and gold. Continuous addition of $HAuCl_4$ to the colloidal solution of silver nanoparticles under heating conditions leads to the change of silver/gold ratio in the nanostructure composition during the process of galvanic replacement reaction. It should be noted that this approach allows LSPR tuning within the range of 400 up to 750 nm (Fig. 14), which is enough to use the obtained nanostructures for infrared laser heating upon the cancer cell treatment. Stopping the electrochemical reaction at desired time makes it possible to obtain bimetalic nanoparticles with different sizes and morphology.

9. Conclusions

Although basically all reviewed approaches for LSPR tuning are based on changing the physical and chemical properties of the environment near the nanoparticle or the physical properties of the nanoparticle itself, such as size, shape and material, the methods of implementing these approaches differ significantly. The main differences are related to simplicity and efficiency of the LSPR tuning techniques, which result in their popularity among researchers. This review describes the use of only chemical, electrochemical and mechanical approaches to the spectral regulation of LSPR, although there are also less commonly used biological, biochemical and optical methods. The presented material can be useful when using LSPR tuning both in scientific research and in the development of new devices using nanoplasmonic technology.

References

1. Chopra K., Paulson P. and Dutta V. Thin-film solar cell: an overview. *Prog. Photovolt.: Res. Appl.* 2004. **12**. P. 69–92. https://doi.org/10.1002/pip.541.

2. Green M. The path to 25% silicon solar cell efficiency: History of silicon cell evolution. *Prog. Photovolt.: Res. Appl*. 2009. **17**. P. 183–189. https://doi.org/10.1002/pip.892.
3. Delbos S. Kesterite thin films for photovoltaics: a review. *EPJ Photovolt.* 2012. **3**. P. 35004p1–35004p13. http://dx.doi.org/10.1051/epjpv/2012008.
4. Schorr S., Hoebler H.-J. and Tovar M. A neutron diffraction study of the stannite-kesterite solid solution series. *Eur. J. Mineralogy*. 2007. **19**. P. 65–73. http://doi.org/10.1127/0935-1221/2007/0019-0065.
5. Patel K.K., Shah D.V. and Kherajl V. Effects of annealing on structural properties of copper zinc tin sulphide (CZTS) material. *Journal of Nano and Electronic Physics*. 2013. **5**, No 2. P. 02031 (3 p.). http://nbuv.gov.ua/UJRN/jnep_2013_5_2_33.
6. Wei M., Du Q., Wang D., Liu W., Jiang G., and Zhu C. Synthesis of spindle-like kesterite Cu_2ZnSnS_4 nanoparticles using thiorea as sulfur source. *Mater. Lett*. 2012. **79**. P. 177–179. https://doi.org/10.1016/j.matlet.2012.03.080.
7. Zhou Y., Zhou W., Du Y.F. and Wu S. Sphere-like kesterite Cu_2ZnSnS_4 nanoparticles synthesized by a facile solvothermal method. *Mater. Lett*. 2011. **56**. P. 1535–1537. https://doi.org/10.1016/j.matlet.2011.03.013.
8. Mirzayev M.N., Abdurakhimov B.A., Demir E. *et al.* Investigation of the formation of defects under fast neutrons and gamma irradiation in 3C–SiC nano powder. *Physica B*. 2021. **611**. P. 412842–412849. https://doi.org/10.1016/j.physb.2021.412842.
9. Fernandes P.A., Salomé P.M.P. and da Cunha A.F. Study of polycrystalline Cu_2ZnSnS_4 films by Raman scattering. *J. Alloys Compds*. 2011. **509**. P. 7600–7606. https://doi.org/10.1016/j.jallcom.2011.04.097.
10. Pareek D., Balasubramaniam K. and Sharma P. Synthesis and characterization of bulk Cu_2ZnSnX_4 (X: S, Se) *via* thermodynamically supported mechano-chemical process. *Mater. Charact*. 2015. **103**. P. 42–49. https://doi.org/10.1016/j.matchar.2015.03.014.
11. Himmrich M., Haeuseler H. Far infrared studies on stannite and wurtzstannite type compounds. *Spectrochim. Acta A*. 1991. **47**. P. 933–942. https://doi.org/10.1016/0584-8539(91)80283-O.
12. Khadka D.B. and Kim J.H. Structural transition and band gap tuning of $Cu_2(Zn,Fe)SnS_4$ chalcogenide for photovoltaic application. *J. Phys. Chem. C*. 2014. **118**. P. 14227–14237. https://doi.org/10.1021/jp503678h.
13. Fernandes P.A., Salome P.M.P. and da Cunha A.F. Growth and Raman scattering characterization of Cu_2ZnSnS_4 thin films. *Thin Solid Films*. 2009. **517**. P. 2519–2523. https://doi.org/10.1016/j.tsf.2008.11.031.
14. Schneider J. and Kirby R.D. Raman scattering from ZnS polytypes. *Phys. Rev. B*. 1972. **6**, No 4. P. 1290–1294. https://doi.org/10.1103/PhysRevB.6.1290.
15. Redinger A., Berg D.M., Dale P.J. and Siebentritt S. The consequences of kesterite equilibria for efficient solar cells. *J. Am. Chem. Soc.* 2011. **133**, No 10. P. 3320–3323. https://doi.org/10.1021/ja111713g.
16. Weber A., Mainz R., and Schock H.W. On the Sn loss from thin films of the material system Cu–Zn–Sn–S in high vacuum. *J. Appl. Phys*. 2010. **107**, No 1. P. 013516(1–6). https://doi.org/10.1063/1.3273495.
17. Timmo K., Altosaar M., Raudoja J. *et al*. Sulfur-containing $Cu_2ZnSnSe_4$ monograin powders for solar cells. *Solar Energy Materials and Solar Cells*. 2010. **94**, No 11. P. 1889–1892. https://doi.org/10.1016/j.solmat.2010.06.046.
18. Xie M., Zhuang D., Zhao M. *et al.* Fabrication of Cu_2ZnSnS_4 thin films using a ceramic quaternary target. *Vacuum*. 2014. **101**. P. 146–150. https://doi.org/10.1016/j.vacuum.2013.08.001.
19. Lee J.H., Choi H.J., Kim W.M. *et al.* Effect of pre-annealing on the phase formation and efficiency of CZTS solar cell prepared by sulfurization of Zn/(Cu,Sn) precursor with H_2S gas. *Solar Energy*. 2016. **136**, No 15. P. 499–504. https://doi.org/10.1016/j.solener.2016.07.031.
20. Katagiri H., Jimbo K., Yamada S. *et al*. Enhanced conversion efficiencies of Cu_2ZnSnS_4-based thin film solar cells by using preferential etching technique. *Appl. Phys. Exp*. 2008. **1**. P. 041201. https://doi.org/10.1143/APEX.1.041201.
21. Maurya D.K., Sikarwar S., Chaudhary P., Angaiah S. and Yadav B.C. Synthesis and characterization of nanostructured copper zinc tin sulphide (CZTS) for humidity sensing applications. *IEEE Sensors J.* 2019. **19**, No 8. P. 2837–2846. http://doi.org/10.1109/JSEN.2018.2890309.
22. Das K., Panda S.K., Gorai S., Mishra P. and Chaudhuri S. Effect of Cu/In molar ratio on the microstructural and optical properties of microcrystalline $CuInS_2$ prepared by solvothermal route. *Mater. Res. Bull*. 2008. **43**, No 10. P. 2742–2750. http://doi.org/10.1016/j.materresbull.2007.10.013.
23. Patel M., Mukhopadhyay I., Ray A. Structural, electrical and optical properties of spray deposited CZTS thin films in non-equilibrium growth condition. *J. Phys. D: Appl. Phys*. 2012. **45**. P. 445103. http://doi.org/10.1088/0022-3727/45/44/445103.
24. Gorai S., Ganguli D. and Chaudhuri S. Synthesis of copper sulfides of varying morphologies and stoichiometries controlled by chelating and nonchelating solvents in a solvothermal process. *Cryst. Growth Des*. 2005. **5**, No 3. P. 875–877. http://doi.org/10.1021/cg0496787.

Authors and CV

Petro V. Demydov, PhD student at the Department of Functional Transducers for Sensor Technology of the V. Lashkaryov Institute of Semiconductor Physics, NAS of Ukraine. His research interests include localized surface plasmon resonance, nanoparticles, electrical and optoelectronic engineering, computational modeling of optical properties of disordered and ordered plasmonic nanosystems based on highly-conductive metallic nanostructures.
ORCID: 0000-0002-8394-5573; vodimed@ukr.net

Andrii M. Lopatynskyi, PhD in Physics and Mathematics, Senior Researcher at the Department of Functional Transducers for Sensor Technology, V. Lashkaryov Institute of Semiconductor Physics, NAS of Ukraine. His research interests include development, experimental investigation, and computational modeling of optical properties of disordered and ordered plasmonic nanosystems based on noble metal nanostructures as well as development of sensor devices on their basis.
ORCID: 0000-0002-6847-892X; lop2000@ukr.net

Illja Igorovych Hudzenko, PhD student at the Department of Functional Transducers for Sensor Technology of the V. Lashkaryov Institute of Semiconductor Physics, NAS of Ukraine. His research interests include localized surface plasmon resonance, surface enchanced fluorescence, plasmon regulated energy transfer in multidomain optical active molecules, plasmonic nanosystems, based on highly-conductive metallic nanostructures.
ORCID: 0000-0002-2212-3891
hudzenkoii@gmail.com

Volodymyr I. Chegel, DSc in Physics and Mathematics, Leading Researcher, Head of Plasmonics group in the Department of Functional Transducers for Sensor Technology at the V. Lashkaryov Institute of Semiconductor Physics, National Academy of Sciences of Ukraine and Professor at Taras Shevchenko National University of Kyiv. His research interests are focused on plasmonics, nanotechnology, materials science, biological and chemical sensors, design of optoelectronic devices.
ORCID: 0000-0002-0190-9932

Поточний стан регуляції хвильової позиції локалізованого поверхневого плазмонного резонансу. Короткий огляд.

П.В. Демидов, А.М. Лопатинський, І.І. Гудзенко, В.І. Чегель

Анотація. Унікальною особливістю наночастинок з високопровідних матеріалів (плазмонні наночастинки) є той факт, що їх хвильову позицію локалізованого поверхневого плазмонного резонансу (ЛППР) можна регулювати, змінюючи форму, розмір, склад і оточуюче середовище відповідно до цілей застосування. У даному огляді наведено приклади основних механізмів регуляції ЛППР, доступних на даний час. Серед найбільш вживаних методів регуляції хвильової позиції ЛППР – використання різного типу матеріалів наночастинок – золота, срібла, міді, алюмінію та сплаву золото-срібло. Також наведено приклади зміни резонансної позиції поглинання шляхом використання наночастинок з різною формою та розмірністю. Розглянуто використання менш вживаних методів регуляції ЛППР, таких як контрольована регуляція відстані між частинками в одному і двох вимірах. Описано роботи, де хвильову позицію ЛППР регулюють за рахунок зміни оточуючого середовища: товщини підкладки, товщини та діелектричних параметрів шару на поверхні наночастинки. Також розглянуто приклади активного впливу на зміну хвильової позиції ЛППР шляхом прикладання електричного потенціалу та регуляцією плазмових мод.

Ключові слова: локалізований поверхневий плазмонний резонанс, наноструктури золота, наночип, регуляція хвильової позиції ЛППР.